PCCP

PAPER

View Article Online
View Journal | View Issue

Cite this: *Phys. Chem. Chem. Phys.*, 2016, **18**, 6885

Novel porphyrin-preparation, characterization, and applications in solar energy conversion†

Jianfeng Lu,‡[a] Hao Li,‡[a] Shuangshuang Liu,[a] Yu-Cheng Chang,[b] Hui-Ping Wu,[b] Yibing Cheng,[ac] Eric Wei-Guang Diau*[b] and Mingkui Wang*[a]

Received 21st September 2015,
Accepted 22nd January 2016

DOI: 10.1039/c5cp05658f

www.rsc.org/pccp

Porphyrins have been demonstrated as one of the most efficient sensitizers in dye-sensitized solar cells (DSSC). Herein, we investigated a series of porphyrin sensitizers functionalized with various π-spacers, such as phenyl for LD14, thiophene for LW4, thiophene–phenyl for LW5, and 2,1,3-benzothiadiazole (BTD)–phenyl for LW24. Photo-physical investigation by means of time-resolved fluorescence and nanosecond transient absorption spectroscopy revealed an accelerated inner charge transfer in porphyrins containing the BTD–phenyl π-spacer. Implementation of an auxiliary electron-deficient BTD unit to the porphyrin spacer also results in a broad light-harvesting ability extending up to 840 nm, contributing to an enhanced charge transfer character from the porphyrin ring to the anchoring group. When utilized as a sensitizer in DSSCs, the LW24 device achieved a power conversion efficiency of 9.2%, higher than those based on LD14 or LW5 porphyrins (PCE 9.0% or 8.2%, respectively) but lower than that of the LW4 device (PCE 9.5%). Measurements of transient photovoltage decays demonstrate that the LW24 device features the up-shifted potential band edge of the conduction band of TiO_2, but involves serious charge recombination in the dye/TiO_2 interface. The findings provide insights into the molecular structure and the charge-transfer characteristics for designing efficient porphyrin sensitizers for DSSC applications.

Introduction

The emulation of photosynthesis and the efficient and sustainable utilization of solar energy have become some of the greatest scientific challenges in the 21st century. Porphyrins and their derivatives play a vital role in photosynthesis due to their superior light-harvesting ability in the visible spectrum, easily tunable photo- and electrochemistry through the functionalization of the periphery (*meso* and β-positions) as well as the variation of the metal centre.[1] In addition to this, these properties lead to fruitful otptoelectronic applications, such as molecular electronics, solar cells, hydrogen evolution, and so on.[2] Synthetic porphyrins are widely incorporated in prototype dye-sensitized solar cells (DSSCs), in which specifically rationally designed porphyrin sensitizers have afforded top power conversion efficiency (PCE), outperforming the standard Ru–polypyridyl dyes.[3] Most of the highly efficient porphyrin sensitizers have a feature of donor–acceptor conjunction.[4] However, typical D–A porphyrin sensitizers have intense but sharp light absorption in the B (450 nm) and Q (550–650 nm) bands, bereft of absorption around 500–600 nm and beyond 750 nm. In pursuit of panchromatic porphyrin sensitizers, extensive attention has been paid to the modification of the donor and acceptor structure of D–A porphyrins, resulting in variations in optical and photovoltaic properties.[5] Notably, the elongation of π conjugation and loss of symmetry in porphyrin molecules have been recognized to broaden and red shift their absorption bands.[2a] Detailed investigation has shown that porphyrin's optoelectronic properties could be efficiently modulated by adjusting the electronic unit between the porphyrin core and the anchor.[6] This particular unit is termed the conjugating 'spacer' in this study as discussed below. The progress of porphyrin applications in DSSCs over the past few years has evidenced a large contribution from a rational design of spacer groups, including the DSSC PCE record of 13.0% from porphyrin SM315, which incorporates a new spacer by implementing an auxiliary electron-deficient unit of benzothiadiazole (BTD) into a phenyl spacer.[3c] However, it is worth noting that the DSSC PCE dramatically decreased to 2.5% if the spacer was changed from BTD–phenyl to BTD.[7] Furthermore, Palomares *et al.* reported that only a tiny change

[a] *Wuhan National Laboratory for Optoelectronics, School of Optical and Electronic Information, Huazhong University of Science and Technology, 1037 Luoyu Road, Wuhan 430074, P. R. China. E-mail: mingkui.wang@mail.hust.edu.cn; Fax: +86-27-87792225*

[b] *Department of Applied Chemistry and Institute of Molecular Science, National Chiao Tung University, Hsinchu 30010, Taiwan. E-mail: diau@mail.nctu.edu.tw; Fax: +886-3-5723764; Tel: +886-3-5131524*

[c] *Department of Materials Engineering, Monash University, Melbourne, Victoria, 3800, Australia*

† Electronic supplementary information (ESI) available. See DOI: 10.1039/c5cp05658f

‡ J. Lu and H. Li contributed equally.

of single atom in the spacer could have a big influence on porphyrins' properties. They found that the DSSC efficiency can be largely improved from 2.55% to 10.41% by changing BTD–furan to BTD–thiophene.[8] These results expose the crucial role of the spacer's structure in porphyrin sensitizers. Therefore, a modification at the spacer is expected to induce a significant effect on the porphyrin sensitizers' optical, redox, and their photovoltaic properties, suggesting a feasible choice rather than on the donor to modulate the optoelectronic properties of porphyrin sensitizers.[3c–e,7,8] Following this strategy, a bunch of porphyrin sensitizers were developed for DSSCs, showing over 10% PCE.[3d,e] It is also worth noting that the same group could have a distinctly different effect on porphyrin's spectral and photovoltaic properties when placed at different positions, such as donor or acceptor moieties (*i.e.*, two different *meso*-positions). For example, Officer and Gordon demonstrated that the acceptor moiety, which acts as a bridge between the porphyrin and the oxide semiconductor surface, has a stronger interaction with the macrocycle than the donor moiety in such D–A type porphyrins.[9] Wang *et al.* reported that the DSSC performance could be improved by 50% when placing the electron-deficient unit 2,3-diphenylquinoxaline (DPQ) at the acceptor moiety rather than at the donor moiety.[10] On the other hand, there are also extensive works on aryl–ethynyl substituted tetrapyrroles, showing variations in optical and redox properties with variations in the aryl group attached to an ethynyl. For example, by attaching additional potent auxochromes to the donor *meso*-positions, Lin *et al.* also reported highly efficient porphyrin sensitizers covering the near-IR region.[11] We notice that few studies have been done on the relationship between the device properties and the porphyrin structure through the analysis of the photo-induced charge transfer *via* spacers.

Due to the importance of the spacer in porphyrins, we have tested various spacers in D–A structured sensitizers. Consequently, we found that by changing the spacer unit from phenyl to thiophene, the device PCEs could be improved from 9.0% to 9.5%.[12] Therein, thiophene is an electron-rich unit while BTD is an electron-deficient unit. A question still arises about the effect of conjugating spacer units on photo-induced charge transfer in porphyrins. In this article, we report our findings on the conjugating spacer group to the terminal benzoic group that is the determinant in the variations in optical, redox of porphyrins. Four D–A type porphyrin sensitizers differentiated in the conjugating spacers, *i.e.* phenyl (LD14),[13] thiophene (LW4), thiophene–phenyl (LW5) or BTD–phenyl (LW24), were investigated. The selected spacer units possess electron-deficient or rich properties, thus providing significant information to rationally design highly efficient porphyrin sensitizers. We found that with a solely aromatic spacer in these porphyrins, the resulting DSSC presents an improved performance due to an increase of electron-donating ability from phenyl to thiophene. The electron deficient aromatic BTD is more beneficial than electron-rich thiophene as a spacer extending unit.

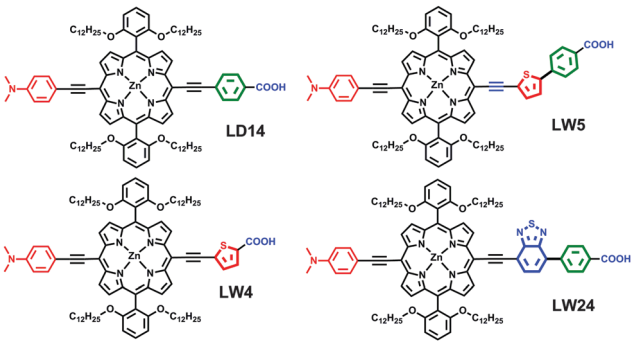

Scheme 1 Molecular structure of the porphyrins LW4, LW5, LW24 and LD14.

Results and discussion

The molecular structures of porphyrin LD14, LW4, LW5, and LW24 are presented in Scheme 1. A rigid anchor structure and a long alkoxyl chain are designed to reduce the recombination reaction induced by molecule aggregation. As shown in Scheme 1, the only difference in the four porphyrin structures is the spacer moiety, aiming to make a clear comparison of spacers in porphyrins. LD14 with phenyl and LW4 with thiophene are supposed to study the influence of spacer's electron-donating ability on the optoelectronic properties of porphyrins and their photovoltaic devices. While the LW5 and LW24 dyes are designed to determine whether an electron-deficient or rich aromatic as a spacer extender is more suitable for DSSCs.

The synthesis of LW24 is summarized in Scheme 2. Unlike the synthesis approach for SM315 or LCVC-series porphyrins as reported by Grätzel and Palomares,[3c,7,8] we introduced

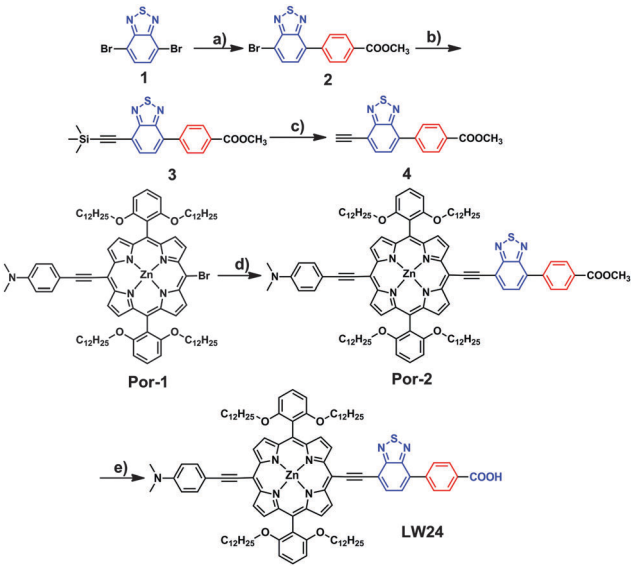

Scheme 2 Synthesis of the LW24 porphyrins: (a) **1**, (4-methoxyphenyl) boronic acid, $Pd(PPh_3)_4$, THF, 2 M K_2CO_3, reflux, overnight; (b) **2**, TMSA, $Pd(OAc)_2$, PPh_3, CuI, THF/TEA, 45 °C, 24 h; (c) **2**, K_2CO_3, MeOH, room temperature, 6 h; (d) **Por-1**, **4**, $Pd(PPh_3)_4$/CuI, THF/TEA, 45 °C, 18 h; (e) (i) **Por-2**, 20% NaOH (aq.), THF, 40 °C, 2 h; (ii) diluted HCl.

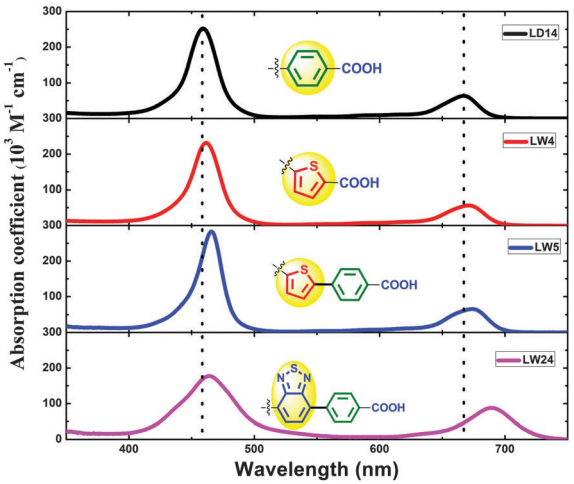

Fig. 1 The absorption spectra of LD14, LW4, LW5, and LW24. All measurements were done in 4×10^{-6} mol L^{-1} in THF solution at 25 °C.

pre-synthesized acceptors to porphyrin at the last step, which has been demonstrated to be an efficient and high purity ensured method.[14] Firstly, 4,7-dibromobenzo[*c*][1,2,5] thiadiazole (compound **1**) was coupled with (4-methoxyphenyl) boronic acid *via* a Pd-catalyzed Suzuki coupling reaction. Then, by treating compound **2** with trimethylsilylacetylene, the Pd-catalyzed Sonogashira coupling reaction was carried out to obtain compound **3**. Later on, compound **4** was achieved in the K_2CO_3/MeOH alkalescence environment. Finally, a standard Sonogashira cross-coupling reaction was applied to synthesize the D–A structured **Por-2**, which was further treated with sodium hydroxide and diluted hydrochloric acid to obtain the final target molecule.

The absorption spectra of these porphyrin dyes are shown in Fig. 1 and the corresponding data are tabulated in Table 1. The resulting dyes exhibit two typical porphyrin B and Q absorption bands at 450–570 and 650–750 nm. The former band involves the transition from the ground state to the second excited state ($S_0 \rightarrow S_2$), while the latter stems from the weaker transition to the first excited state ($S_0 \rightarrow S_1$).[3c] As depicted in Fig. 2a, the Q band of LW4 slightly red-shifts by 4 nm compared to the LD14, originating from the spacer substitution from phenyl to thiophene. For the thiophene–phenyl conjugated LW5, the Q-band red-shifts about 3 nm compared to that of LW4. Indeed, the elongation of π conjugation and loss of symmetry in the porphyrin molecule result in broadened and red shifted absorption bands.[2a] Thus, we can ascribe the red-shift of LW4 (compared to LD14) to the latter reason, and LW5 (compared with LD14 or LW4) to the former. When replacing thiophene (an electron-rich unit) with BTD (an electron-deficient aromatic unit), the Q band dramatically red-shifts by 15 nm from 674 nm for porphyrin LW5 to 689 nm for porphyrin LW24, as presented in Fig. 2b. Otherwise, the Q band maximum molar extinction coefficient of LW24 increases 30% to 8.8×10^4 M^{-1} cm^{-1} compared to LW5 (6.6×10^4 M^{-1} cm^{-1}), indicating a promising application for thin-film DSSCs.[12e] Since the conjugation length of LW5 and LW24 is very similar, the above results suggest that the porphyrin dye's absorption spectrum is greatly dependent on the intrinsic properties of the spacer unit. It also means that a versatile synthesis platform for panchromatic porphyrins could be expected by adjusting the aromatics in the spacer part.

The fluorescence emission maxima of LD14, LW4, LW5 and LW24 dyes in THF solution are found at 684, 687, 691, and 710 nm, showing a mirror image to their Q absorption bands as depicted in Fig. 2c. The increased Stokes shift of LW24 (20 nm for LW24) compared with the other porphyrins (17, 16, and 17 nm for LD14, LW4, and LW5) indicates a strong dipole moment in the excited states of this porphyrin.[15] The bathochromic shift as well as broader PL spectra is an indication of intense charge transfer character within the LW24 porphyrins' excited state. This will be discussed below.

The HOMOs calculated from their first oxidation potentials (E_{ox}) are determined to be −5.22, −5.21, −5.18 and −5.23 eV, while the LUMOs are −3.38, −3.38, −3.36 and −3.45 eV, if we transform the cyclic voltammetry (CV) into the energy level in a vacuum.[16] The HOMO and LUMO values of the LD14 and LW4 porphyrins are identical, while difference in LW5 and LW24 is clearly indicated. It appears that the electron-deficient aromatic unit of BTD shifts the LUMO level negatively, while the electron-rich thiophene unit mainly influences the HOMO level. The distribution of HOMO and LUMO energy levels in such D–A structured porphyrin molecules is largely localized on the donor moiety and the acceptor moiety, respectively.[17] In this case, the variation of energy levels could be explained by assuming the BTD unit serving as an auxiliary acceptor in LW24, while thiophene serving as an auxiliary donor in LW5.

Table 1 Absorption, fluorescence, and first porphyrin-ring redox potential of various porphyrins (LD14, LW4, LW5 and LW24) in THF at 25 °C

Dye	Absorption λ_{max}[a]/nm (10^3/M^{-1} cm^{-1})	Emission[b] λ_{max}/nm	PL[e] lifetime τ/ns	E_{ox}[c]/V (*vs.* NHE)	E_{0-0}[d]/V (*vs.* NHE)	$E_{ox} - E_{0-0}$/V
LD14[f]	459(253.8) 667(64.1)	684	1.69	0.72	1.84	−1.12
LW4	462(234.1) 671(56.4)	687	1.54	0.71	1.83	−1.12
LW5	466(283.1) 674 (65.9)	691	1.66	0.68	1.82	−1.14
LW24	464(177.6) 689(87.8)	710	0.89	0.73	1.78	−1.05

[a] Absorption and emission data were measured in THF at 25 °C. [b] Excitation wavelength/nm: LD14, 459; LW4, 462; LW5, 466; LW24, 464. [c] First porphyrin ring oxidation; electrochemical measurements were performed at 25 °C with each porphyrin (0.5 mM) in THF/0.1 M TBAP/N_2, GC working and Pt counter electrodes, Ag/AgCl reference electrode, scan rate = 50 mV s^{-1}. [d] Estimated from the intersection wavelengths of the normalized UV-vis absorption and the fluorescence spectra. [e] The fluorescence time were measured under a laser excitation of 445 nm. [f] LD14 was synthesized according to literature ref. 13.

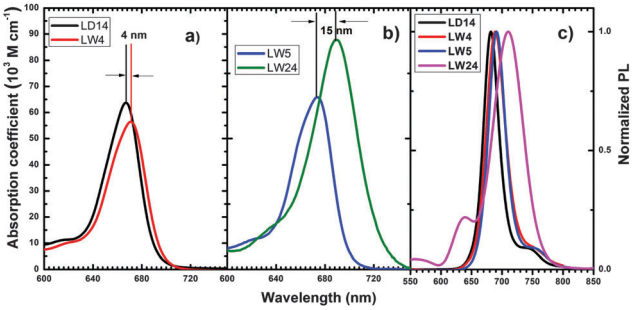

Fig. 2 (a) The Q band absorption spectra of LW4 and LD14; (b) the Q band absorption spectra of LW5 and LW24; (c) the steady-state emission of LD14 LW4, LW5, and LW24. All measurements were done with 4×10^{-6} mol L^{-1} THF solution at 25 °C.

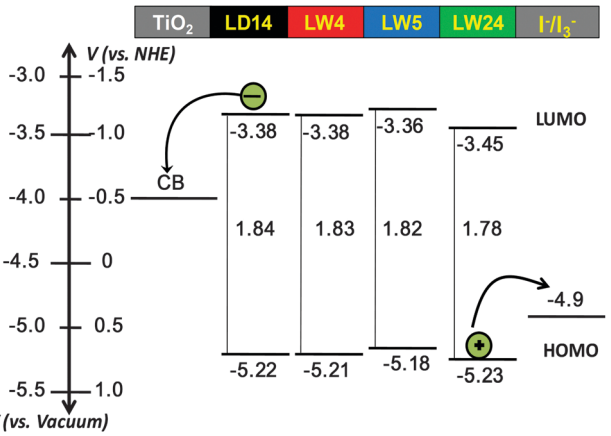

Fig. 3 Energy diagram of the sensitizers LD14, LW4, LW5, LW24, redox couple, and the conduction band of TiO_2. The HOMO and LUMO levels were obtained from the ground state redox potentials and the optical energies. And the difference of the potential for the NHE (U_{redox}) *versus* an electron in a vacuum ($E_{F,redox}$) can be given as: $E_{F,redox}$ [eV] = $-4.5 - eU_{redox}$ [V].[16]

As depicted in Fig. 3, the conduction band of TiO_2 locates at −4.0 eV, while the redox potential of the electrolyte is −4.9 eV.[16] Thus these porphyrins are sufficient to ascertain the injection and regeneration reaction from a thermodynamic point of view (Fig. 2). Density-functional theory (DFT) calculations were also performed on the LD14 and LW4 dyes to gain insight into the electronic structures of their frontier molecular orbitals. As shown in Fig. S5 (ESI†), the HOMOs are localized on the donor (dimethylamine) and macrocycle moieties; in contrast, the LUMOs are highly visible on the macrocycle and the acceptor moieties (π-spacer and carboxyl acid).

Utilizing the time-correlated single photon counting technique, we measured the fluorescence decay lifetime of LD14, LW4, LW5 and LW24 dyes, gaining insights into the electron injection process from the photoexcited porphyrin to the TiO_2 conduction band.[18] Fig. 4 presents the fluorescence decay for the porphyrin dyes in THF and on nanocrystalline TiO_2 films in the presence of electrolytes used in the photovoltaic experiments. In THF solution, the lifetime of the LD14, LW4, LW5 and LW24 dyes is 1.69, 1.54, 1.66 and 0.89 ns (in Table 1). The LW24 porphyrin shows the fastest decay among the tested samples, being nearly

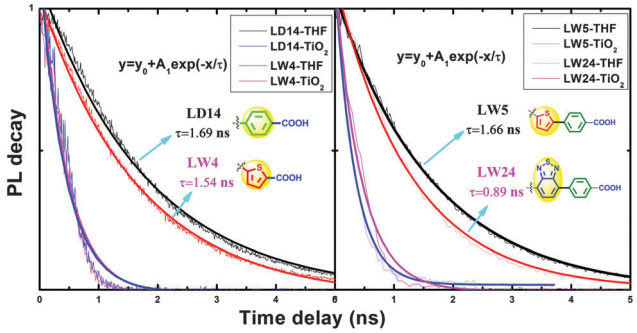

Fig. 4 Time-resolved photoluminescence decay traces of dye-grafted mesoporous titania film and dye in THF solvent. Excitation wavelength: 445 nm, detected at: LD14, 684 nm; LW4, 687 nm; LW5, 691 nm; LW24, 710 nm. The traces with scatter are raw data; the solid curves are the results fitted according to the equation.

half of the other three porphyrins. It confirms a strong electron-coupling of the donor and acceptor in the excited state.[19] When those porphyrins adsorbed onto the TiO_2 nanoparticle surface, a strong quenching of emission was observed. The lifetime of the excited singlet state of LD14, LW4, LW5 and LW24 and LD14 dyes in the adsorbed state is estimated to be about 150 ps. This confirms a rapid electron injection from the excited state of sensitizers into the TiO_2 conduction band.[20]

Nanosecond transient absorption spectrum were performed to scrutinize the dynamics of the recombination of electrons injected in the conduction band of $TiO_2(e_{cb})$ with the oxidized dye (S^+) and that of the dye regeneration reaction with iodide.[21] Fig. 5 shows the transients at 550 nm for the samples on titania in the presence and absence of the redox complex. The pump

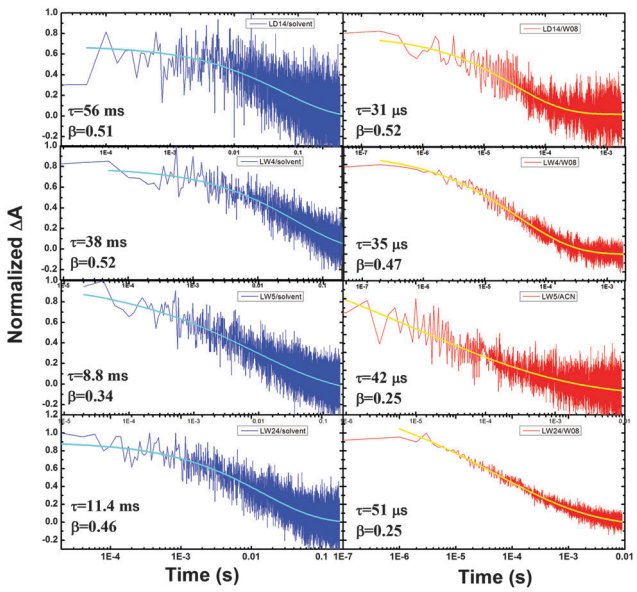

Fig. 5 Transient absorption spectra (TAS) of LD14, LW4, LW5, and LW24 porphyrins on mesoporous TiO_2, with or without redox couple (iodine based electrolyte, coded W08). The traces with scatter are raw data; the solid curves are the results fitted according to the equation. Excitation wavelength: 460 nm; detection wavelength: 550 nm.

Table 2 Parameters of the stretched exponential function used in the fit of the transient absorption signals for various porphyrins (LW4, LW5, LW24 and LD14) on the TiO_2 electrode in the presence and absence of the iodine-based electrolyte. The excitation wavelength is 460 nm and the detective wavelength is 550 nm. τ_1 and β are the parameters acquired from eqn (1), τ_{obs} is the averaged time constant, k_{rec} and k_{reg} are the rate constant of recombination and regeneration process, respectively. φ_{reg} is the quantum yield of the dye regeneration

	ACN			I^-/I_3^-					
Dye	τ_1 (ms)	β	τ_{obs} (ms)	τ_1 (μs)	β	τ_{obs} (μs)	k_{rec} (s^{-1})	k_{reg} (M^{-1} s^{-1})	φ_{reg} (%)
LD14	56	0.51	108	31	0.52	70	9.3	4.7×10^5	99.9
LW4	38	0.52	71	35	0.47	79	14.1	4.2×10^5	99.9
LW5	8.8	0.34	23	42	0.25	1008	43.5	2.9×10^4	95.6
LW24	11.4	0.46	27	51	0.25	1224	37.0	2.4×10^4	95.5

pulses at 460 nm are attenuated with neutral density filters before excitation of the sample with a fluence of less than 40 μJ cm^{-2}. The decays have been fitted by a stretched-exponential function eqn (1) as follows:[21]

$$A(t) = A_n e^{-(t/\tau)\beta} \quad (1)$$

where τ is the characteristic lifetime and β is the stretch parameter ($0 < \beta < 1$, $\beta = 1$ corresponding to a monoexponential decay). Eqn (1) takes into account of the exponential distribution of energy states in the conduction band, the presence of trap states, and the different dye distributions onto the semiconductor surface.[21b] In the devices containing solely inert electrolytes without the redox couple, the electron recombination reaction is only on the interactions between the dye and the electrons located in the conduction band and the trap states of TiO_2. Thus, the extracted lifetimes of LD14, LW4, LW5 and LW24 were estimated to be 56, 38, 8.8 and 11.4 ms as listed in Table 2. In the presence of the redox couple, the oxidized dye molecules are not only reduced by the recombination process, but also by the regeneration process *via* the electrolyte as well. In this case, the acquired lifetimes of LD14, LW4, LW5 and LW24 are 31, 35, 42 and 52 μs. To investigate the non-exponential decay analysis precisely, the average time constants and the averaged rate are calculated according to the literature.[21a,b]

In this configuration, the rate constants (k_{rec}) for the recombination process calculated from the inverse of the recombination average time constants are 9.3, 14.1, 43.5 and 37.0 s^{-1} for LD14, LW4, LW5 and LW24, respectively. Thus, the regeneration rate constant, k_{reg}, can be obtained by using eqn (2) with the previously calculated value k_{rec} for the recombination:

$$k_{reg} = \frac{k_{obs} - k_{rec}}{[I^-]} \quad (2)$$

where the $[I^-]$ refers to the concentration of the reduced species of the redox pair. The k_{reg} calculated from eqn (2) are 4.7×10^5, 4.2×10^5, 2.9×10^4 and 2.4×10^2 s^{-1}. The obviously slower oxidized dye regeneration rate of LW5 and LW24 could be explained by the longer conjugation length of molecules. Considering the different results from PL decay and TAS, it suggested different charge transfer processes from porphyrin sensitizers to the semiconductor or to reduction species in the presence of an electrolyte. Table 2 gives the obtained rate constants for the cells sensitized with LD14, LW4, LW5 and LW24. Finally, the quantum yield of the dye regeneration (φ_{reg}) for the complete device is determined from eqn (3):[21]

$$\varphi(\text{reg}) = \frac{k_{reg}[I^-]}{k_{obs}} \quad (3)$$

As shown in Table 2, the oxidized dye regeneration efficiencies are 99.9%, 99.9%, 95.6% and 95.5% for LD14, LW4, LW5 and LW24 devices, respectively. It is worth noting that the porphyrins (LW5 and LW24) featuring a longer π spacer (thiophene–phenyl or BTD–phenyl) exhibit a slightly lower value of regeneration efficiency than that having shorter ones (phenyl or thiophene).

The driving force of the regeneration reaction can be informed from the difference of the electrolyte's redox potential and the dye's HOMO level. As illustrated in Fig. 3, it is evaluated to have similar driving force values of 0.32, 0.31, 0.28, and 0.33 eV for the LD14, LW4, LW5, and LW24, respectively. Therefore, we can conclude that the variation in φ_{reg} is not induced by the thermodynamic driving force.[22] Generally, regeneration of the oxidized dye in the homogeneous medium can be reasonably well described by the classic theory of electron transfer developed by Marcus.[21c] Within this context, all the investigated porphyrins are designed with the same donor and the porphinate group. We may ascribe the different rate of electron transfer between the donor and the acceptor to the variation of the conjugation length and intrinsic properties of the spacer. As presented in Table 2, it is likely that an identical φ_{reg} could be found for these dyes possessing a similar conjugation length as evidenced in LW5 and LW24, or LD14 and LW4. Furthermore, the result infers that the conjugation length has a critical influence on the regeneration reaction in porphyrin based DSSC systems, rather than their intrinsic properties of those units. Thus, the regeneration is quite similar for the porphyrins with similar spacer length regardless of the electron-deficient or rich units inserted between porphine and benzoic acid.

By using an optimized binary solvent of toluene and ethanol (volume ratio 1 : 1), the porphyrins were sensitized onto a bilayer (7.5 + 5.0 μm) titania film to serve as a working electrode. We evaluated these porphyrins in DSSC devices in combination with the iodine-based electrolyte. The current–voltage (J–V) characteristics and the corresponding action spectra of incident photons to electrons conversion efficiency (IPCE) of the devices are shown in Fig. 6a and b. The photovoltaic parameters, *i.e.*, PCE, short circuit photocurrent density (J_{SC}), the open circuit photovoltage (V_{OC}), and fill factor (FF) extracted from Fig. 6a are summarized in Table 3. The LD14 devices show a PCE 9.01% with a V_{OC} 734 mV, while LW4 devices exhibit 9.53% with a superior V_{OC} of 751 mV. The better performance of the latter is mainly benefited from the higher V_{OC}. However, for LW5, the J_{SC} of the corresponding devices decrease nearly 2 mA cm^{-2}, in spite of an enhanced light-harvesting ability around 725–750 nm. For LW24 featuring the BTD extended spacer, the IPCE tail of the corresponding devices significantly broadens to nearly 840 nm. Thus, the LW24 DSSC

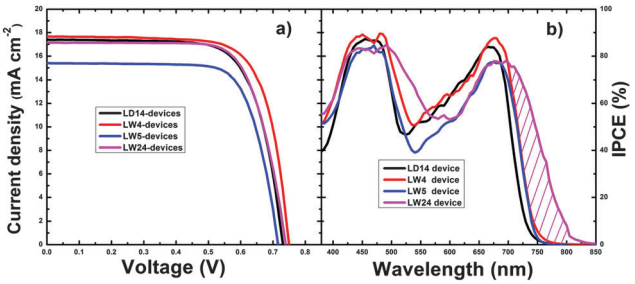

Fig. 6 (a) J–V curves of and the DSSC devices based on LD14, LW4, LW5, and LW24 porphyrins measured under simulated AM 1.5G full sunlight; (b) IPCE spectra of LD14, LW4, LW5, and LW24 porphyrins devices. The cells were measured with a mask (area = 0.09 cm^{-2}).

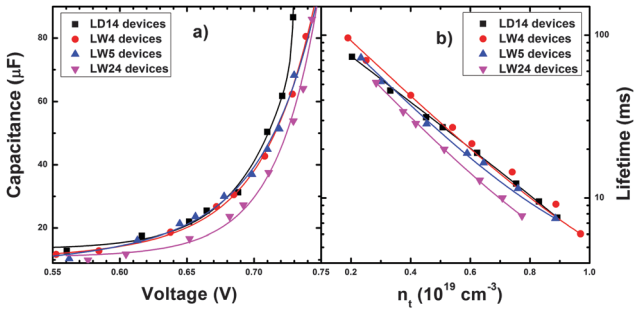

Fig. 7 Transient photovoltage decay and charge extraction measurements of LD14, LW4, LW5, and LW24 based DSSC devices. (a) Comparisons of chemical capacitance at a certain open–circuit photovoltage; (b) comparisons of electron lifetime at a given electron density.

Table 3 Photovoltaic parameters (with standard deviations) of DSSC devices using LD14, LW4, LW5, and LW24 dyes in combination with the iodine-based electrolyte under an irradiation at 100 mW cm^{-2}. Five independent cells were measured to obtain the average values. The cells were measured using a mask (area = 0.09 cm^{-2})

Device	J_{SC} (mA cm^{-2})	V_{OC} (V)	FF	PCE (%)
LD14	17.38 ± 0.10	0.734 ± 0.006	0.710 ± 0.002	9.01 ± 0.06
LW4	17.65 ± 0.18	0.751 ± 0.008	0.720 ± 0.003	9.53 ± 0.07
LW5	15.41 ± 0.12	0.719 ± 0.004	0.735 ± 0.005	8.16 ± 0.10
LW24	17.14 ± 0.20	0.737 ± 0.012	0.723 ± 0.012	9.21 ± 0.12

devices achieve a J_{SC} of 17.14 mA cm^{-2}. LW24 devices not only show a higher PCE than LW5 devices, but also superior than LD14. The IPCE intensity is a function of charge collection, electron injection in TiO_2, and dye regeneration efficiency.[22] As discussed above, the oxidized dye regeneration efficiencies of LW5 or LW24 are lower than LD14 or LW4, which may give a clue for the lower IPCE values in the former two kinds of devices.

The V_{OC} value is defined as the energy difference between the quasi-Fermi level (E_F) of the TiO_2 under illumination and the Nernst potential of the redox electrolyte ($E_{F,redox}$).[22] Since all the devices here utilize similar electrolytes, TiO_2 photoanodes and fabrication processes, the variations of V_{OC} can be rationalized and explained based on the changes of electronic E_F, which depends on the electron density in the TiO_2.[23] In this case, we performed transient photo-voltage decay and charge extraction measurements to understand the physical origin of the V_{OC} difference between the four porphyrin based DSSCs.[24] Fig. 7a presents the capacitance (C_μ) at different voltages for various DSSCs. The C_μ value follows the expression of $C_\mu \propto \exp(qV/mkT)$,[25] where k is the Boltzmann constant, T is the absolute temperature, and m is related to the shape of the distribution of the density of states. Similar slopes for the plots in Fig. 7a indicate the same trap state distribution in TiO_2 for various devices. At the identical C_μ, the open-circuit voltage of LW24 device is about 10–20 mV higher than the other devices (Fig. 7a). Whilst the LD14 devices show a slight 5 mV lower than LW4 and LW5 devices, and 15 mV lower than LW24. Sensitizers adsorbed on the semiconductor surface can modify its electronic properties, such as band bending, on account of different dipole moments ($\Delta\varphi \propto N\mu\cos\theta$, where $\Delta\varphi$ is the electrostatic potential drop, N being the number of adsorbed molecules per surface area, μ being the molecular dipole moment, θ being the tilt angle between the axes of the dipole moment and the surface normal of the TiO_2 particles).[26] Neglecting the amount and tilt angle of the four porphyrins adsorbed on TiO_2,[27] it is likely that the higher TiO_2 band bending edge in LW24 devices could be explained by the bigger dipole moment of LW24 porphyrin. Fig. 7b presents the electron lifetime (τ) as a function of electron density, which further provides information about the recombination between the injected electrons in TiO_2 and the oxidized form of electrolytes.[3] All devices showed a similar shape of the curves in Fig. 7b, which may be ascribed to the efficient insulation of the TiO_2 surface by the same four dodecyloxy-chains.[28] At a given electron density, the electron lifetime of LW4 device is longer than the other three porphyrins, while the LW24 device is the shortest one. The BTD group can accelerate conduction-band electron recapture by the sensitizer.[3b,c,7] Thus, we ascribe the lower V_{OC} of LW24 in comparison with LW4 devices to a serious recombination reaction.

Conclusions

In summary, we have shown a systematic investigation of the influence of various π-spacers in porphyrin sensitizers on the photo-induced charge transfer process and photovoltaic performance. The results reveal that the electron-deficient unit BTD inserted between the porphyrin core and the benzoic acid anchoring group could lead to a broadened light-harvesting spectral region as well as an upward shift of the conduction band edge of TiO_2. However, the electron-rich unit thiophene at the same site shows a less significant impact. These results could be explained by the difference of electron coupling in the excited state as well as internal charge transfer within the molecule. Porphyrins with a solely aromatic spacer show a prolonged electron lifetime and a faster dye-regeneration reaction in comparison with the spacer extended porphyrins. The compromised effect brought about by the extension of the conjugation length results in the overall conversion efficiency of 9.2% for LW24, while LW4 with a shorter spacer presented the highest efficiency of 9.5%. We believe that this structure–property relationship will shed light on better molecular design

and synthesis of panchromatic porphyrin sensitizers to further improve the photovoltaic performance of a DSSCs.

Acknowledgements

JL, HL, SL, YC, and MW thank the Director Fund of WNLO, the 973 Program of China (2014CB643506 and 2013CB922104) and NSFC (21173091) for financial support; they also thank the Analytical and Testing Centre at HUST for performing characterization of various samples. YCC, HPW and EWGD received support from National Chiao Tung University (NCTU), Ministry of Science and Technology (MOST) of Taiwan and Ministry of Education (MOE) of Taiwan. The authors also thank Prof. Jie Xu for the DFT calculation results. JL thanks NCTU (Hsinchu, Taiwan) and WNLO (Wuhan, China) for supporting his visit to NCTU.

Notes and references

1 T. Hasobe, H. Imahori, P. Kamat, T. Ahn, S. Kim, D. Kim, A. Fujimoto, T. Hirakawa and S. Fukuzumi, *J. Am. Chem. Soc.*, 2005, **127**, 1216–1228.

2 (*a*) H. Imahori, T. Umeyama and S. Ito, *Acc. Chem. Res.*, 2009, **42**, 1809–1818; (*b*) L.-L. Li and E. W.-G. Diau, *Chem. Soc. Rev.*, 2013, **42**, 291–304; (*c*) M. Urbani, M. Grätzel, M. K. Nazeeruddin and T. Torres, *Chem. Rev.*, 2014, **114**, 12330–12396; (*d*) T. Higashino and H. Imahori, *Dalton Trans.*, 2015, **44**, 448–463; (*e*) J. Kesters, P. Verstappen, M. Kelchtermans, L. Lutsen, D. Vanderzande and W. Maes, *Adv. Energy Mater.*, 2015, **5**, 1500218; (*f*) D. Huang, J. Lu, S. Li, Y. Luo, C. Zhao, B. Hu, M. Wang and Y. Shen, *Langmuir*, 2014, **30**, 6990–6998.

3 (*a*) T. Bessho, S. Zakeeruddin, C.-Y. Yeh, E. W.-G. Diau and M. Grätzel, *Angew. Chem., Int. Ed.*, 2010, **49**, 6646–6649; (*b*) A. Yella, H. Lee, H. Tsao, C. Yi, A. Chandiran, M. Nazeeruddin, E. W.-G. Diau, C.-Y. Yeh, S. Zakeeruddin and M. Grätzel, *Science*, 2011, **334**, 629–634; (*c*) M. Mathew, A. Yella, P. Humphry-Baker, B. Curchod, N. Ashari-Astani, I. Tavernelli, U. Rothlisberger, M. Nazeeruddin and M. Grätzel, *Nat. Chem.*, 2014, **6**, 242–247; (*d*) Y. Xie, Y. Tang, W. Wu, Y. Wang, J. Liu, X. Li, H. Tian and W. Zhu, *J. Am. Chem. Soc.*, 2015, **137**, 14055–14058; (*e*) C.-L. Wang, M. Zhang, Y.-H. Hsiao, C.-K. Tseng, C.-L. Liu, M. Xu, P. Wang and C.-Y. Lin, *Energy Environ. Sci.*, 2016, **9**, 200–206.

4 (*a*) C.-W. Lee, H.-P. Lu, C.-M. Lan, Y.-L. Huang, Y.-R. Liang, W.-N. Yen, Y.-C. Liu, Y.-S. Lin, E. W.-G. Diau and C.-Y. Yeh, *Chem. – Eur. J.*, 2009, **15**, 1403–1412; (*b*) W. Li, Z. Liu, H. Wu, Y. Cheng, Z. Zhao and H. He, *J. Phys. Chem. C*, 2015, **119**, 5265–5273; (*c*) W. Li, L. Si, Z. Liu, Z. Zhao, H. He, K. Zhu, B. Moore and Y. Cheng, *J. Mater. Chem. A*, 2014, **2**, 13667–13674.

5 (*a*) K. Kurotobi, Y. Toude, K. Kawamoto, Y. Fujimori, S. Ito, P. Chabera, V. Sundstrçm and H. Imahori, *Chem. – Eur. J.*, 2013, **19**, 17075–17081; (*b*) M. Ishida, D. Hwang, Z. Zhang, Y. Choi, J. Oh, V. Lynch, D. Kim, J. Sessler and D. Kim, *ChemSusChem*, 2015, **8**, 2967–2977; (*c*) Y. Wang, B. Chen, W. Wu, X. Li, W. Zhu, H. Tian and Y. Xie, *Angew. Chem., Int. Ed.*, 2014, **53**, 10779–10783; (*d*) F. Jradi, D. O'Neil, X. Kang, J. Wong, P. Szymanski, T. Parker, H. Anderson, M. El-Sayed and S. Marder, *Chem. Mater.*, 2015, **27**, 6305–6313.

6 (*a*) K. Ladomenou, T. Kitsopoulos, G. Sharma and A. Coutsolelos, *RSC Adv.*, 2014, **4**, 21379–21404; (*b*) M. Sreenivasu, A. Suzuki, M. Adachi, C. Kumar, B. Srikanth, S. Rajendar, D. Rambabu, R. Kumar, P. Mallesham, N. Bhaskar Rao, M. Kumar and P. Reddy, *Chem. – Eur. J.*, 2014, **20**, 14074–14083.

7 A. Yella, C.-L. Mai, S. Zakeeruddin, S.-N. Chang, C.-H. Hsieh, C.-Y. Yeh and M. Grätzel, *Angew. Chem., Int. Ed.*, 2014, **126**, 3017–3021.

8 L. Cabau, C. Kumar, A. Moncho, J. Clifford, N. López and E. Palomares, *Energy Environ. Sci.*, 2015, **8**, 1368–1375.

9 H. Salm, S. Lind, M. Griffith, P. Wagner, G. Wallace, D. Officer and K. Gordon, *J. Phys. Chem. C*, 2015, **119**, 22379–22391.

10 S. Fan, K. Lv, H. Sun, G. Zhou and Z. Wang, *J. Power Sources*, 2015, **279**, 36–47.

11 (*a*) C.-H. Wu, M.-C. Chen, P.-C. Su, H.-H. Kuo, C.-L. Wang, C.-Y. Lu, C.-H. Tsai, C.-C. Wu and C.-Y. Lin, *J. Mater. Chem. A*, 2014, **2**, 991–999; (*b*) J. Luo, M. F. Xu, R. Z. Li, K. W. Huang, C. Y. Jiang, Q. B. Qi, W. D. Zeng, J. Zhang, C. Y. Chi, P. Wang and J. S. Wu, *J. Am. Chem. Soc.*, 2014, **136**, 265–272; (*c*) Q. Qi, R. Li, J. Luo, B. Zhang, K. Huang, P. Wang and W. Wu, *Dyes Pigm.*, 2015, **122**, 199–205; (*d*) J.-W. Shiu, Y.-C. Chang, C.-Y. Chan, H.-P. Wu, H.-Y. Hsu, C.-L. Wang, C.-Y. Lin and E. W.-G. Diau, *J. Mater. Chem. A*, 2015, **3**, 1417–1420.

12 (*a*) J. Lu, X. Xu, K. Cao, J. Cui, Y. Zhang, Y. Shen, X. Shi, L. Liao, Y. Cheng and M. Wang, *J. Mater. Chem. A*, 2013, **1**, 10008–10015; (*b*) J. Lu, B. Zhang, S. Liu, H. Yuan, Y. Shen, Y. Cheng, J. Xu and M. Wang, *Phys. Chem. Chem. Phys.*, 2014, **16**, 24755–24762; (*c*) J. Lu, S. Liu, H. Li, Y. Shen, Y. Cheng, J. Xu and M. Wang, *J. Mater. Chem. A*, 2014, **2**, 17495–17501; (*d*) J. Lu, B. Zhang, H. Yuan, X. Xu, K. Cao, J. Cui, S. Liu, Y. Shen, Y. Cheng, J. Xu and M. Wang, *J. Phys. Chem. C*, 2014, **118**, 14739–14748; (*e*) J. Lu, Y.-C. Chang, H.-Y. Cheng, H.-P. Wu, Y. Cheng, M. Wang and E. W.-G. Diau, *ChemSusChem*, 2015, **8**, 2529–2536.

13 Y.-C. Chang, C.-L. Wang, T.-Y. Pan, S.-H. Hong, C.-M. Lan, H.-H. Kuo, C.-F. Lo, H.-Y. Hsu, C.-Y. Lin and E. W.-G. Diau, *Chem. Commun.*, 2011, **47**, 8910–8912.

14 (*a*) J. Lu, X. Xu, Z. Li, K. Cao, J. Cui, Y. Zhang, Y. Shen, Y. Li, J. Zhu, S. Dai, W. Chen, Y. Cheng and M. Wang, *Chem. – Asian J.*, 2013, **8**, 956–962; (*b*) J. Lu, S. Liu, Y. Shen, J. Xu, Y. Cheng and M. Wang, *Electrochim. Acta*, 2015, **179**, 187–196.

15 S. Haid, M. Marszalek, A. Mishra, M. Wielopolski, J. Teuscher, J. Moser, R. Humphry-Baker, S. Zakeeruddin, M. Grätzel and P. Bäuerle, *Adv. Funct. Mater.*, 2012, **22**, 1291–1302.

16 (*a*) M. Grätzel, *Nature*, 2001, **414**, 338–344; (*b*) A. Hagfeldt, G. Boschloo, L. Sun, K. Kloo and H. Pettersson, *Chem. Rev.*, 2010, **114**, 6595–6663; (*c*) M. Wang, C. Grätzel, S. Zakeeruddin and M. Grätzel, *Energy Environ. Sci.*, 2012, **5**, 9394–9405.

17 (*a*) X. Gu and Q. Sun, *Phys. Chem. Chem. Phys.*, 2013, **15**, 15434–15440; (*b*) T. Wei, X. Sun, X. Li, H. Ågren and Y. Xie, *ACS Appl. Mater. Interfaces*, 2015, **7**, 21956–21965.

18 (*a*) R. Katoh and A. Furube, *J. Photochem. Photobiol., C*, 2014, **20**, 1–16; (*b*) R. Milot and C. Schmuttenmaer, *Acc. Chem. Res.*, 2015, **48**, 1423–1431.

19 A. Margalias, K. Seintis, M. Yigit, M. Can, D. Sygkridou, V. Giannetas, M. Fakis and E. Stathatos, *Dyes Pigm.*, 2015, **121**, 316–327.

20 L.-Y. Luo, R. Ambre, S. Mane, E. Diau and C. Hung, *Phys. Chem. Chem. Phys.*, 2015, **17**, 20134–20143.

21 (*a*) A. Anderson, P. Barnes, J. Durrant and B. O'Regan, *J. Phys. Chem. C*, 2011, **115**, 2439–2447; (*b*) P. Piatkowski, C. Martin, M. Nunzio, B. Cohen, S. Pandey, S. Hayse and S. Douhal, *J. Phys. Chem. C*, 2014, **118**, 29674–29687; (*c*) S. Feldt, G. Wang, G. Boschloo and H. Hagfeldt, *J. Phys. Chem. C*, 2011, **115**, 21500–21507.

22 A. Yella, R. Humphry-Baker, B. Curchod, N. Astani, J. Teuscher, L. Polander, S. Mathew, J. Moser, I. Tavernelli, U. Rothlisberger, M. Grätzel, M. Nazeeruddin and J. Frey, *Chem. Mater.*, 2013, **25**, 2733–2739.

23 A. Reynal, A. Forneli, E. Martinez-Ferrero, A. Sanchez-Diaz, A. Vidal-Ferran, B. O'Regan and E. Palomares, *J. Am. Chem. Soc.*, 2008, **130**, 13558–13567.

24 (*a*) L.-L. Li, Y.-C. Chang, H.-P. Wu and E. W.-G. Diau, *Int. Rev. Phys. Chem.*, 2012, **31**, 420–467; (*b*) M. Griffith, K. Sunahara, P. Wagner, K. Wagner, G. Wallace, D. Officer, A. Furube, R. Katoh, S. Mori and A. Mozer, *Chem. Commun.*, 2012, **48**, 4145–4162.

25 S. Jang, K. Zhu, M. Ko, K. Kim, C. Kim, N. Park and A. Frank, *ACS Nano*, 2011, **5**, 8267–8274.

26 S. Rühle, M. Greenshtein, S. Chen, A. Merson, H. Pizem, C. Sukenik, D. Cahen and A. Zaban, *J. Phys. Chem. B*, 2005, **109**, 18907–18913.

27 (*a*) S. Ye, A. Kathiravan, H. Hayashi, Y. J. Tong, Y. Infahsaeng, P. Chabera, T. Pascher, A. Yartsev, S. Isoda, H. Imahori and V. Sundström, *J. Phys. Chem. C*, 2013, **117**, 6066–6080; (*b*) H. Hayashi, T. Higashino, Y. Kinjo, Y. Fujimori, K. Kurotobi, P. Chabera, V. Sundström, S. Isoda and H. Imahori, *ACS Appl. Mater. Interfaces*, 2015, **7**, 18689–18696.

28 C.-L. Wang, J.-Y. Hu, C.-H. Wu, H.-H. Kuo, Y.-C. Chang, Z.-J. Lan, H.-P. Wu, E. W.-G. Diau and C.-Y. Lin, *Energy Environ. Sci.*, 2014, **7**, 1392–1396.

